### RESEARCH ARTICLE

#### **PHYSICS**

# **Quantum control of trapped polyatomic molecules** for eEDM searches

Loïc Anderegg<sup>1,2</sup>\*, Nathaniel B. Vilas<sup>1,2</sup>, Christian Hallas<sup>1,2</sup>, Paige Robichaud<sup>1,2</sup>, Arian Jadbabaie<sup>3</sup>, John M. Doyle<sup>1,2</sup>, Nicholas R. Hutzler<sup>3</sup>\*

Ultracold polyatomic molecules are promising candidates for experiments in quantum science and precision searches for physics beyond the Standard Model. A key requirement is the ability to achieve full quantum control over the internal structure of the molecules. In this work, we established coherent control of individual quantum states in calcium monohydroxide (CaOH) and demonstrated a method for searching for the electron electric dipole moment (eEDM). Optically trapped, ultracold CaOH molecules were prepared in a single quantum state, polarized in an electric field, and coherently transferred into an eEDM-sensitive state where an electron spin precession measurement was performed. To extend the coherence time, we used eEDM-sensitive states with tunable, near-zero magnetic field sensitivity. Our results establish a path for eEDM searches with trapped polyatomic molecules.

he rich structure of polyatomic molecules makes them an appealing platform for experiments in quantum science (1-4), ultracold chemistry (5), and precision measurements (6-10). Key to this structure is the presence of near-degenerate states of opposite parity, which allow the molecules to be easily polarized in the laboratory frame with the application of a small electric field. Such states are generic among polyatomic molecules, but rare in diatomics, and may be useful for applications such as analog simulation of quantum magnetism models (1, 2) or for realizing switchable interactions and long-lived qubit states for quantum computing (4). Additionally, the parity-doublet states in trapped polyatomic molecules are expected to be an invaluable tool for systematic error rejection in precision measurements of physics beyond the Standard Model (BSM) (6). To date, several species of polyatomic molecules have been laser cooled and/or trapped at ultracold temperatures (11-17).

One powerful avenue for tabletop BSM searches is probing for the electron electric dipole moment (eEDM) (18-22),  $d_{\rm e}$ , which violates time-reversal (T) symmetry and is predicted by many BSM theories to be orders-of-magnitude larger than the Standard Model prediction (19, 20). Present state-of-the-art eEDM experiments are broadly sensitive to T-violating physics at energies much greater than 1 TeV (23-28). All such experiments use Ramsey spectroscopy to measure an energy shift caused by the interaction of the electron

with the large electric field that is present inside a polarized molecule (24–26, 27, 29). Molecular beam experiments have achieved high statistical sensitivity by measuring a large number of molecules over a  $\approx$ 1-ms coherence time (24, 25), whereas molecular ion-based experiments have used long Ramsey interrogation times ( $\approx$ 1 s), though with lower numbers (26, 27, 29). Measurements with trapped neutral polyatomic molecules can potentially combine the best features of each approach to achieve orders-of-magnitude improved statistical sensitivity (6).

## Experimental approach for polyatomic molecule control

In this work, we demonstrate full quantum control over the internal states of a trapped polyatomic molecule in a vibrational bending mode with high polarizability in small electric fields. The protocol starts with preparing ultracold, optically trapped molecules in a single hyperfine level, after which a static electric field is applied to polarize the molecules. The strength of the polarizing electric field is tuned to obtain near-zero g-factor spin states, which have strongly suppressed sensitivity to magnetic field noise while retaining eEDM sensitivity. Microwave pulses are applied to create a coherent superposition of these zero g-factor spin states, which precesses under the influence of an external magnetic field. The precession phase is then read out by a combination of microwave pulses and optical cycling.

We observed spin precession over a range of electric and magnetic fields and characterized the present limitations to the coherence time of the measurement. With readily attainable experimental parameters, coherence times on the order of the state lifetime (>100 ms) could be realistically achieved. We therefore realized the key components of an eEDM measure-

ment in this system. Note that eEDM sensity arises from the relativistic motion of electron, which is enhanced by higher-mass nuclei. Although the light mass of CaOH precludes a competitive eEDM measurement (30), the protocol demonstrated here is directly transferable to heavier laser-cooled alkaline earth monohydroxides with identical internal level structures, such as SrOH, YbOH, and RaOH, which have substantially enhanced sensitivity to the eEDM (6, 11, 12, 30, 31).

In eEDM measurements with polarized molecules, the electron spin  $\vec{S}$  precesses under the influence of an external magnetic field  $B_Z$  and the internal electric field of the molecule  $E_{\rm eff}$  which can be large owing to relativistic effects. Time evolution is described by the Hamiltonian

$$H = g_{\rm S} \mu_{\rm B} B_Z \vec{S} \cdot \hat{Z} - d_{\rm e} E_{\rm eff} \vec{S} \cdot \hat{n}$$

$$= g_{\rm S} \mu_{\rm B} B_Z M_{\rm S} - d_{\rm e} E_{\rm eff} \Sigma \tag{1}$$

Here,  $g_{\rm S}\approx 2$  is the electron spin g-factor,  $\mu_{\rm B}$  is the Bohr magneton,  $B_Z$  points along the lab  $\hat{Z}$  axis, and the internal field  $E_{\rm eff}$  points along the molecule's internuclear axis  $\hat{n}$ . We define the quantities  $M_{\rm S}=\vec{S}\cdot\hat{Z}$  and  $\Sigma=\vec{S}\cdot\hat{n}$  to describe the electron's magnetic sensitivity and EDM sensitivity, respectively. The effect of the eEDM can be isolated by switching the orientation of the applied magnetic field or, alternatively, by switching internal states to change the sign of  $M_{\rm S}$  or  $\Sigma$ . Performing both switches is a powerful technique for suppressing systematic errors (25,26).

Present EDM bounds rely on specific states in diatomic molecules that have an unusually small g-factor, which reduces sensitivity to stray magnetic fields (24, 26). However, CaOH, like other laser-coolable molecules with structure amenable to eEDM searches (6, 31-33), has a single valence electron, which results in large magnetic g-factors. In this work, we engineered reduced magnetic sensitivity by using an applied electric field  $E_Z$  to tune  $M_S$  to a zerocrossing while maintaining substantial eEDM sensitivity  $\Sigma$ . This technique is generic to polyatomic molecules with parity doublets. Details of a specific  $M = \pm 1$  pair of zero g-factor states are shown in Fig. 1, A and B, with further information provided in (34). We emphasize that near the zero g-factor crossing, the eEDM sensitivity is nearly maximal because of the large projection of the electron spin onto the internal electric field of the molecule. Sensitivity to transverse magnetic fields is also suppressed in these zero g-factor states (34).

## Experimental overview and single-state preparation

The experiment begins with laser-cooled CaOH molecules loaded from a magneto-optical trap (14) into an optical dipole trap (ODT) formed by a 1064-nm laser beam with a 25-µm waist

<sup>&</sup>lt;sup>1</sup>Department of Physics, Harvard University, Cambridge, MA 02138, USA. <sup>2</sup>Harvard-MIT Center for Ultracold Atoms, Cambridge, MA 02138, USA. <sup>3</sup>Division of Physics, Mathematics, and Astronomy, California Institute of Technology, Pasadena, CA 91125, USA.

<sup>\*</sup>Corresponding author. Email: anderegg@g.harvard.edu (L.A.); hutzler@caltech.edu (N.R.H.)

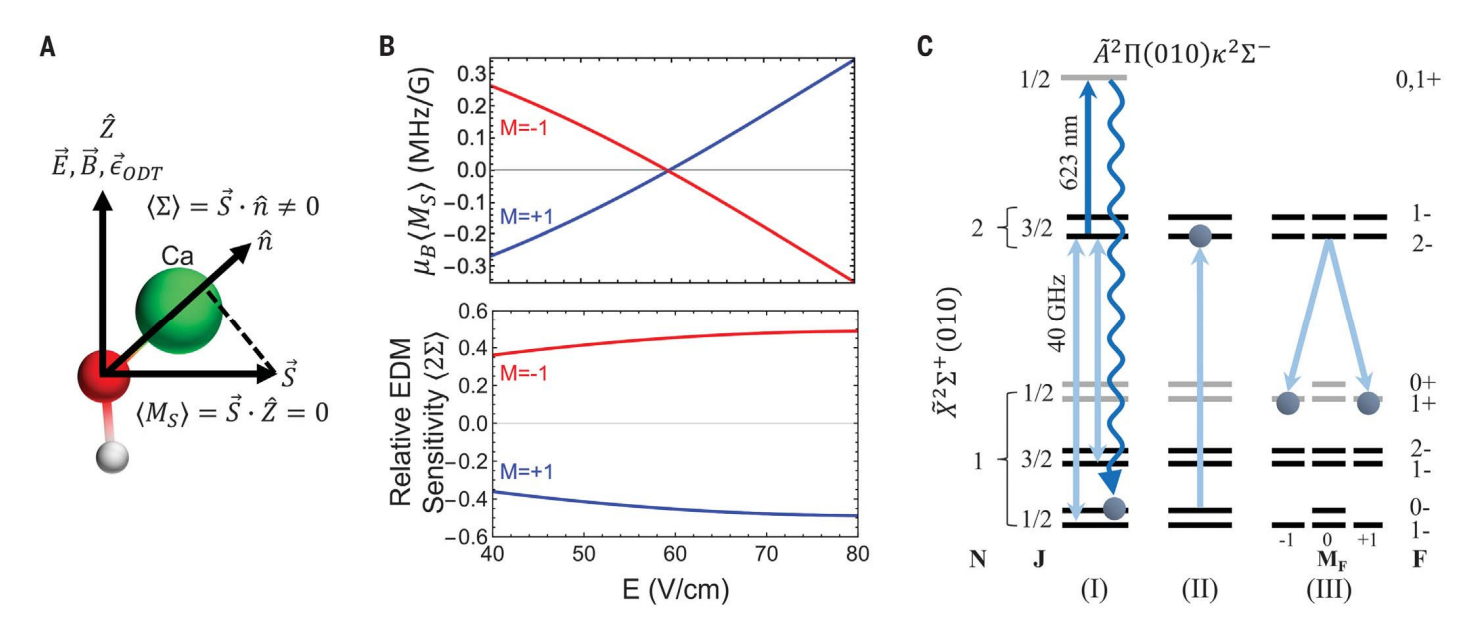


Fig. 1. Overview of the experiment. (A) A geometric picture of the bending molecule at the zero g-factor crossing, showing that the electron spin (S) has a finite projection on the molecule axis  $(\hat{n})$ , giving eEDM sensitivity. However, the electron spin (S)is orthogonal to the magnetic field (B), which results in suppressed magnetic field sensitivity. (B) The magnetic sensitivity (top) and eEDM sensitivity (bottom) for a pair of zero g-factor states (N = 1,  $J = 1/2^+$ , F = 1,  $M_F = \pm 1$ ) are shown as a function of the applied electric field. (C) Experimental sequence to prepare the

eEDM-sensitive state. First, the molecules are pumped into a single quantum state  $(N = 1, J = 1/2^-, F = 0)$  with a combination of microwave drives and optical pumping (I). Next, a microwave  $\pi$ -pulse drives the molecules into the N=2,  $J=3/2^-$ , F=2,  $M_{\rm F}$  = 0 state (II). Lastly, the eEDM measurement state is prepared as a coherent superposition of the N=1,  $J=1/2^-$ , F=1,  $M_F=\pm 1$  states with a microwave  $\pi$ -pulse (III). The states that are optically detectable with the detection light are shown in black, whereas those not addressed by the detection light are in gray.

size, as described in previous work (15). The ODT is linearly polarized, and its polarization vector  $\vec{\epsilon}_{\text{ODT}}$  defines the  $\hat{Z}$  axis, along which we also apply magnetic and electric fields, B = $B_Z\hat{Z}$  and  $E=E_Z\hat{Z}$ , respectively, as depicted in Fig. 1A. We first nondestructively image the molecules in the ODT for 10 ms as normalization against variation in the number of trapped molecules. The molecules are then optically pumped into the  $N = 1^-$  levels of the  $\tilde{X}^2 \Sigma^+$  (010) vibrational bending mode (15) (Fig. 1C), and the trap depth is adiabatically lowered by 3.5 times to reduce the effect of ac Stark shifts from the trap light and to lower the temperature of the molecules to 34 µK. Any molecules that were not pumped into  $N = 1^-$  levels of the bending mode are heated out of the trap with a pulse of resonant laser light.

After transfer to the  $\tilde{X}^2\Sigma^+(010)(N=1^-)$ state, the molecular population is initially spread across 12 hyperfine Zeeman sublevels in the spin-rotation components J = 1/2 and 3/2. To prepare the molecules in a single hyperfine state, we used a combination of optical pumping and microwave pulses, as shown in Fig. 1C. We first applied microwaves from the N = 1.  $J = 3/2^{-}$  state up to the N = 2,  $J = 3/2^{-}$  state. Because this transition is parity-forbidden, we applied a small electric field  $E_Z = 7.5 \text{ V/cm}$  to slightly mix the parity of the N = 1 levels and provide transition strength. From the N = 2state, we drove an optical transition to the excited  $\tilde{A}^2\Pi(010)\kappa^2\Sigma^{(-)}, J=1/2^+$  state. This state predominately decays to both the F = 0

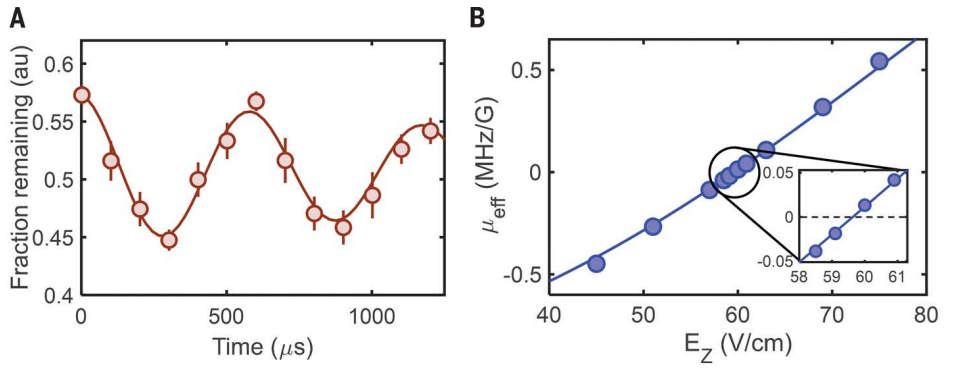


Fig. 2. Spin precession. (A) Spin precession of the eEDM-sensitive state in the presence of a bias magnetic field. Error bars represent 68% confidence intervals. au, arbitrary units. (B) Magnetic-field sensitivity of the eEDM state in CaOH as a function of electric field. The field sensitivity is determined by measuring the spin-precession frequency at different electric fields with an applied magnetic field of  $B_Z = 110$  mG. Error bars are smaller than the markers. The solid curve is the calculated magnetic-field sensitivity in the presence of trap shifts using known molecular parameters (34).

(the target state) and F=1 states in the N=1,  $J = 1/2^-$  manifold. After 3 ms of optical pumping, the microwaves were switched to drive the accumulated N = 1,  $J = 1/2^-$ , F = 1 population to the same N = 2, J =  $3/2^-$  state in X(010), where they are excited by the optical light and pumped into the target F = 0 state. Once this optical pumping sequence is complete, we adiabatically ramped the electric field to  $E_Z$  = 150 V/cm to substantially mix parity, then drove the population up to the N = 2, J = $3/2^-$ , F = 2, M = 0 state with a microwave  $\pi$ -pulse (Fig. 1C, II). We cleaned out any remaining population in the N = 1 state with a depletion laser that resonantly drives the population to undetected rotational levels.

#### Spin precession in an eEDM-sensitive state

To perform spin precession in the eEDMsensitive state, we first adiabatically ramped the electric field to a value  $E_Z$ , then turned on a small bias magnetic field  $B_Z$ . We measured the electron spin precession frequency using a procedure analogous to Ramsey spectroscopy (24, 25). The molecules were prepared by driving a  $\pi$ -pulse (2.5  $\mu$ s), with microwaves linearly

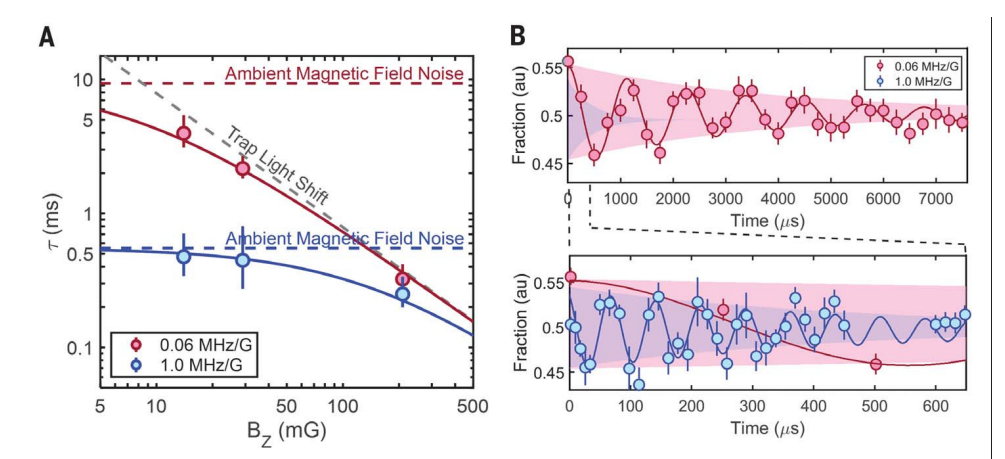
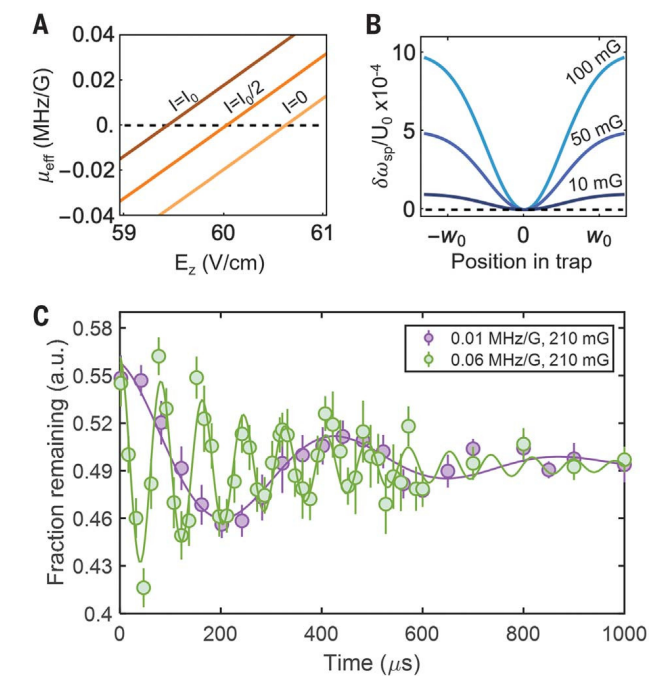


Fig. 3. Coherence time of the spin-precession signal. (A) Measured coherence times  $\tau$  versus  $B_Z$  at different electric fields (red and blue markers, which correspond to different magnetic field sensitivities). The coherence time scales as  $1/B_Z$  owing to ac Stark-shift broadening then plateaus at a limit set by the magnetic field instability δB. This limit increases as the g-factor approaches zero. Solid and dashed curves are fit to the data. The ambient magnetic field noise determined from the fit is  $\delta B = 4^{+2}_{-1}\,\text{mG}$ , and the fitted decoherence time due to light shifts is  $\tau = (1/B_Z) \times 80^{+20}_{-10}$  ms  $\times$  mG. (**B**) Spin-precession signal, at  $B_Z$  = 15 mG, near the zero g-factor crossing (0.06 MHz/G; red) and far from the crossing (1.0 MHz/G; blue). Shaded regions indicate the fitted exponential decay envelope of the oscillations; the 1.0 MHz/G data are excluded from the top panel for clarity. The spin-precession coherence time is extended by 16 times by approaching the zero g-factor point.

Fig. 4. Effect of trap light on coherence time. (A) Effective magnetic moment,  $\mu_{\text{eff}}$ , as a function of electric field for several trap intensities I. The trap light shifts the location of the zero crossing in  $\mu_{\text{eff}}$ . As a result, molecules at a finite temperature explore different magnetic-field sensitivities  $\mu_{\text{eff.}}$  (B) Dependence of the spin-precession frequency (scaled by the trap depth  $U_0$ ) on the position within the trap, where  $w_0$  is the trap waist. At lower magnetic fields, the relative change in spinprecession frequency is reduced. (C) Two spin-precession curves taken at the same magnetic field  $(B_7 = 210 \text{ mG})$  but at different electric fields, showing that the ac Stark-shift limitation is independent of the effective g-factor because ac Stark shifts dominate the coherence time for large bias fields.



polarized along the lab  $\hat{X}$  axis, into the "bright" superposition state  $|B\rangle = (|M=1\rangle + |M=-1\rangle)/$  $\sqrt{2}$  within the  $N = 1, J = 1/2^+, F = 1, M = \pm 1$ eEDM-sensitive manifold (Fig. 1C, III). The state begins to oscillate between the bright state and the "dark" state  $|D\rangle = (|M=1\rangle - |M=1\rangle)$  $-1\rangle)/\sqrt{2}$  at a rate  $\omega_{\rm SP}$ =  $\mu_{\rm eff}B_Z$ , where the effective magnetic moment  $\mu_{eff} = \mu_B g_{eff} = g_E \mu_B$  $(\langle M_{
m S} 
angle_{M=1} - \langle M_{
m S} 
angle_{M=-1})$  is tuned by means of the applied electric field  $E_Z$  (Fig. 1B). The contribution from the  $d_{\rm e}E_{\rm eff}$  term in Eq. 1 is negligible in CaOH but could be measured in heavier molecules with much larger  $E_{\rm eff}$ . After a given time, a second  $\pi$ -pulse was applied to stop spin precession and transfer the bright state to the optically detectable  $N = 2, J = 3/2^{-1}$ level. Once the electric field was ramped down, the population remaining in the eEDM manifold, which has the opposite parity, is not optically detectable. We then imaged the ODT again and took the ratio of the first and second images (Fig. 2A). At long spin precession times

(>10 ms), losses from background gas collisions (~1 s), blackbody excitation (~1 s), and the spontaneous lifetime of the bending mode (~0.7 s) lead to an overall loss of signal, as characterized in (15). This effect is mitigated with a fixed duration between the first and second images, making the loss independent of the precession time.

To map out the location of the zero g-factor crossing, we performed spin precession measurements at a fixed magnetic field  $B_Z$  = 110 mG for different electric fields (Fig. 2B). The spin precession frequency corresponds to an effective g-factor at that electric field. We found that the zero *g*-factor crossing within the N = 1,  $J = 1/2^+, F = 1, M = \pm 1$  eEDM manifold occurs at an electric field of 59.6 V/cm, in agreement with theory calculations described in (34). We note that there is another zero g-factor crossing for the  $N=1, J=3/2^+, F=1$  manifold at ≈64 V/cm, which has a smaller eEDM sensitivity but the opposite slope of  $g_{\text{eff}}$  versus  $E_Z$ , thereby providing a powerful resource to reject systematic errors related to imperfect field reversals (34). We emphasize that although the location of these crossings is dependent on the structure of a specific molecule, their existence is generic in polyatomic molecules, which naturally have parity-doublet structure (6).

#### **Coherence time and limitations**

A critical component of the spin precession measurement is the coherence time, which sets the sensitivity of an eEDM search. Figure 3A shows the measured coherence time of our system at different applied fields  $B_Z$  and  $E_Z$ . We characterized two dominant limitations that wash out oscillations at long times. Variations in the spin precession frequency can be linearly expanded as  $\delta \omega_{SP} = \mu_{eff}(\delta B_Z) +$  $(\delta \mu_{\rm eff})B_Z$ . The first term describes magnetic field noise and drift of the applied bias field, given by  $\delta B_Z$ . The second term describes noise and drifts in the g-factor,  $\delta g_{\text{eff}}$ , which can arise from instability in the applied electric field,  $E_Z$ , or from ac Stark shifts (described below). Drifts in the bias electric field  $E_Z$  were found to be negligible in our apparatus.

Decoherence caused by magnetic field noise,  $\delta B_{Z_3}$  is independent of the applied magnetic field but is proportional to  $\mu_{eff}$  and can be mitigated by operating near the zero g-factor crossing. As shown in Fig. 3B, at an electric field of 90 V/cm, corresponding to a large magnetic moment of  $\mu_{eff}$  = 1.0 MHz/G, we realized a magnetic field noise-limited coherence time of 0.5 ms at  $B_Z \approx 15$  mG (blue points). At an electric field of 61.5 V/cm, corresponding to  $\mu_{eff}$  = 0.06 MHz/G, which is much closer to the zero g-factor location, we found a coherence time of 4 ms at the same  $B_Z$  (red points in Fig. 3B).

At higher magnetic fields, the primary limitation to the coherence time is ac Stark shifts from the optical trapping light (Fig. 4). The intense Z-polarized ODT light leads to a shift

in the electric field at which the zero g-factor crossing occurs. Owing to the finite temperature of the molecules within the trap, they will explore different intensities of trap light and hence have different values of  $g_{\text{eff}}$ . The spread  $\delta g_{\rm eff}$  causes variation of  $\omega_{\rm SP}$ , which leads to decoherence. In contrast to the magnetic field noise term, this effect is independent of the electric field  $E_Z$  but decreases monotonically with  $B_Z$ , which scales the frequency sensitivity to g-factor variations,  $\delta\omega_{\rm SP}$  =  $B_Z\delta\mu_{\rm eff}$ . The insensitivity of g-factor broadening to the exact value of  $g_{\rm eff}$  is demonstrated in Fig. 4C. Decoherence caused by ac Stark shifts can be reduced by cooling the molecules to lower temperatures or by decreasing  $B_Z$ . The bias magnetic field can be reduced arbitrarily far until either transverse magnetic fields or magnetic field noise becomes dominant. From the decoherence rates measured in this work, it is expected that ac Stark shift-limited coherence times of ~1 s could be achieved at bias fields of  $B_Z \sim 100 \,\mu\text{G}$ .

From the above discussion, it is expected that the longest achievable coherence times will occur for very small g-factors,  $g_{\text{eff}} \approx 0$ , and very small bias fields,  $B_Z \approx 0$ . Minimizing  $B_Z$ requires reducing the effects of both magnetic field noise and transverse magnetic fields to well below the level of the bias-field energy shifts. We canceled the transverse magnetic fields to below 1 mG by maximizing the spin precession period under the influence of transverse B fields only, and actively monitored and fed back on the magnetic field along each axis to minimize noise and drifts in  $B_Z$ . Note that the stainless-steel vacuum chamber has no magnetic shielding, which leads to high levels of magnetic field noise that would not be present in an apparatus designed for an eEDM search. Even under these conditions, we achieved a coherence time of 30 ms at an electric field of 60.3 V/cm (corresponding to  $\mu_{eff}$  = 0.02 MHz/G) and a bias field of  $B_Z \approx 2$  mG (34). However, at such a low bias field, the molecules are sensitive to 60-Hz magnetic field noise that is present in the unshielded apparatus, which is on the same order as the bias field. Because the experiment is phase-stable with respect to the ac line frequency, this 60-Hz magnetic field fluctuation causes a time-dependent spin precession frequency. Nevertheless, our prototype experiment confirms that long coherence times are possible. Any future eEDM experiment would have magnetic shielding that would greatly suppress nefarious magnetic fields from the environment. Such shielding could readily enable coherence times that exceed that of the ~0.5-s lifetime of the bending modes of similar linear polyatomic molecules with larger eEDM sensitivity (15).

#### Discussion and outlook

We have realized coherent control of optically trapped polyatomic molecules and demonstra-

ted a realistic experimental roadmap for future eEDM measurements. By leveraging the distinctive features of the quantum levels in polyatomic molecules, we achieved a coherence time of 30 ms for paramagnetic molecules in a stainless-steel chamber with no magnetic shielding. With common shielding techniques used in past EDM experiments, there is a clear path to reducing stray fields and extending coherence times to >100 ms. At such a level, the dominant limitation becomes the finite lifetime of the bending mode (15). Even longer coherence times are possible with the right choice of parity-doublet states, as found in symmetric or asymmetric top molecules (6, 13, 35, 36).

Following this roadmap with heavier trapped polyatomic molecules has the potential to provide orders-of-magnitude improvements to present bounds on T-violating physics. Using a recent study of the X(010) state in YbOH (37), we identified similar N = 1 zero g-factor states for eEDM measurements with greatly improved sensitivity. In addition to the g-factor tuning demonstrated in this work, polyatomic molecules provide the ability to reverse the sign of  $\Sigma$  without reversing  $M_S$ , which is a crucial feature of recent experiments that has greatly improved the limit on the eEDM (25, 27). For example, in the N=1 manifold of CaOH, there is another zero g-factor crossing at a nearby electric field value, with 69% smaller values of  $\Sigma$  and opposite sign. Because the ratio of eEDM sensitivity to g-factor versus  $E_Z$  slope differs between these two crossings, measurements at both points could be used to suppress systematics caused by nonreversing fields that couple to the electric field dependence of the g-factor (25).

This work provides an experimental demonstration of the advantages of the rich level structure of polyatomic molecules for precision measurements. Although we focused here on spin precession with T-reversed states (M =±1), many levels of interest can be favorably engineered for precision measurement experiments. In a recent proposal (9), parity doublets, magnetically tuned to degeneracy in optically trapped polyatomic molecules, were shown to be advantageous for searches for parityviolating physics. In another recent work (7), a microwave clock between rovibrational states in SrOH was proposed as a sensitive probe of ultralight dark matter, by using transitions tuned to electric and/or magnetic insensitivity. In these proposals, and as now experimentally demonstrated in our work, coherent control and state engineering in polyatomic molecules can mitigate systematic errors and enable robust searches for new physics.

#### REFERENCES AND NOTES

- M. L. Wall, K. Maeda, L. D. Carr, Ann. Phys. 525, 845-865 (2013).
- M. Wall, K. Maeda, L. D. Carr, New J. Phys. 17, 025001 (2015).
- Q. Wei, S. Kais, B. Friedrich, D. Herschbach, J. Chem. Phys. 135, 154102 (2011).

- 4. P. Yu, L. W. Cheuk, I. Kozyryev, J. M. Doyle, New J. Phys. 21, 093049 (2019)
- L. D. Augustovičová, J. L. Bohn, New J. Phys. 21, 103022
- 6. I. Kozyryev, N. R. Hutzler, Phys. Rev. Lett. 119, 133002 (2017).
- I. Kozyryev, Z. Lasner, J. M. Doyle, Phys. Rev. A 103, 043313 (2021)
- 8. N. R. Hutzler, Quantum Sci. Technol. 5, 044011 (2020).
- E. B. Norrgard et al., Commun. Phys. 2, 77 (2019).
- 10. Y. Hao et al., Phys. Rev. A 102, 052828 (2020).
- 11. I. Kozyryev et al., Phys. Rev. Lett. 118, 173201 (2017).
- 12. B. L. Augenbraun et al., New J. Phys. 22, 022003 (2020).
- 13. D. Mitra et al., Science 369, 1366-1369 (2020).
- 14. N. B. Vilas et al., Nature 606, 70-74 (2022).
- 15. C. Hallas et al., Phys. Rev. Lett. 130, 153202 (2023).
- 16. M. Zeppenfeld et al., Nature 491, 570-573 (2012).
- 17. A. Prehn, M. Ibrügger, R. Glöckner, G. Rempe, M. Zeppenfeld, Phys. Rev. Lett. 116, 063005 (2016).
- 18. D. DeMille, J. M. Doyle, A. O. Sushkov, Science 357, 990-994
- 19. T. E. Chupp, P. Fierlinger, M. J. Ramsey-Musolf, J. T. Singh, Rev. Mod. Phys. 91, 015001 (2019).
- 20. M. S. Safronova et al., Rev. Mod. Phys. 90, 025008 (2018)
- 21. C. Cesarotti, O. Lu. Y. Nakai, A. Parikh, M. Reece, J. High Energy Phys. 2019, 59 (2019).
- 22. M. Pospelov, A. Ritz, Ann. Phys. 318, 119-169 (2005).
- 23. J. J. Hudson et al., Nature 473, 493-496 (2011).
- 24. J. Baron et al., Science 343, 269-272 (2014)
- 25. ACME Collaboration, Nature 562, 355-360 (2018)
- 26. W. B. Cairncross et al., Phys. Rev. Lett. 119, 153001 (2017). 27. T. S. Roussy et al., Science 381, 46-50 (2023).
- 28. R. Alarcon et al., arXiv:2203.08103 [hep-ph] (2022).
- 29. Y. Zhou et al., Phys. Rev. Lett. 124, 053201 (2020).
- 30. K. Gaul, R. Berger, Phys. Rev. A 101, 012508 (2020).
- 31. T. A. Isaev, A. V. Zaitsevskii, E. Eliav, J. Phys. At. Mol. Opt. Phys **50**, 225101 (2017).
- 32. T. A. Isaev, R. Berger, Phys. Rev. Lett. 116, 063006 (2016).
- 33. I. Kozyryev, L. Baum, K. Matsuda, J. M. Doyle, ChemPhysChem 17, 3641-3648 (2016).
- 34. See supplementary materials.
- 35. B. L. Augenbraun, J. M. Doyle, T. Zelevinsky, I. Kozyryev, Phys. Rev. X 10, 031022 (2020).
- 36. B. L. Augenbraun et al., Phys. Rev. A 103, 022814 (2021).
- 37. A. Jadbabaie et al., New J. Phys. 25, 073014 (2022).
- 38. L. Anderegg et al., Data for quantum control of trapped polyatomic molecules for eEDM searches. Zenodo (2023); https://doi.org/10.5281/zenodo.8384389.

#### **ACKNOWLEDGMENTS**

A.J. acknowledges helpful discussions with C. Zhang and P. Yu. Funding: This work was supported by the Air Force Office of Scientific Research and the National Science Foundation (NSF). L.A. acknowledges support from the Harvard Quantum Initiative. N.B.V. from the Department of Defense National Defense Science and Engineering Graduate fellowship program, and P.R. from the NSF Graduate Research Fellowship Program. N.R.H. and A.J. acknowledge support from NSF CAREER program (PHY-1847550), the Gordon and Betty Moore Foundation (GBMF7947), and the Alfred P. Sloan Foundation (G-2019-12502). Author contributions: L.A., N.B.V., C.H., P.R., and A.J. performed the experiment and analyzed the data, N.R.H. and J.M.D. directed the study. All authors discussed the results and contributed to the manuscript. Competing interests: None declared. Data and materials availability: All data needed to evaluate the conclusions in this paper are present in the paper or in the supplementary materials. All data presented in this paper are deposited at Zenodo (38). License information: Copyright @ 2023 the authors, some rights reserved; exclusive licensee American Association for the Advancement of Science. No claim to original US government works. https://www.science.org/about/sciencelicenses-iournal-article-reuse

#### SUPPLEMENTARY MATERIALS

science.org/doi/10.1126/science.adg8155 Supplementary Text Figs. S1 to S4 References (39-50)

Submitted 23 January 2023; accepted 29 September 2023 10.1126/science.adg8155



#### Quantum control of trapped polyatomic molecules for eEDM searches

Loïc Anderegg, Nathaniel B. Vilas, Christian Hallas, Paige Robichaud, Arian Jadbabaie, John M. Doyle, and Nicholas R. Hutzler

Science 382 (6671), . DOI: 10.1126/science.adg8155

#### **Editor's summary**

Cold molecules hold much promise as a platform for investigating fundamental problems in physics such as matter-antimatter asymmetry through precise measurements of the electron's electric dipole moment (eEDM). Researchers have used diatomic molecules for this purpose. Polyatomic molecules have even more favorable properties but are more difficult to control. Anderegg *et al.* demonstrate coherent control of individual quantum states in the polyatomic molecule calcium monohydroxide. Their findings enable the measurement of eEDM in this and related systems, which is expected to lead to improved precision. —Jelena Stajic

#### View the article online

https://www.science.org/doi/10.1126/science.adg8155

https://www.science.org/help/reprints-and-permissions

Use of this article is subject to the Terms of service